Proceedings of the 17th World Congress
The International Federation of Automatic Control
Seoul, Korea, July 6-11, 2008

Explicit Nonlinear MPC of an Automotive Electromechanical Brake

Chih Feng Lee [1] **Chris Manzie** **Chris Line**

Research Centre for Advanced By-Wire Technologies (RABiT)
Department of Mechanical Engineering
The University of Melbourne, Victoria 3010, Australia.

Abstract: Electromechanical brakes (EMB) have great potential for automotive applications due to performance, manufacturing and environmental benefits. One key performance criterion is the ability to track brake clamp forces requested by higher level controllers such as anti-lock braking and electronic stability systems. Prior EMB controllers have utilised architectures including cascaded proportional-integral (PI) control and linear model predictive control (MPC), although only with suboptimal results. In this paper, an explicit nonlinear constrained MPC is proposed for the EMB. The explicit control law is obtained by minimising a quadratic performance criterion. The solution is computed offline and saved to memory to avoid the computational expense of online optimisation. The control law is implemented in simulation using a lookup table and its effectiveness is demonstrated. The effect of model parameter variation on control performance is discussed, and its impact on the controller implementation is investigated with a view to determining the most suitable parameters for online adaptation. Model parameter adaptation within the explicit MPC framework is also investigated.

1. INTRODUCTION

Amidst the rapid development of advanced microelectronic and electrical actuator technologies, microcontroller based computer, communication and actuation systems are becoming less expensive, more powerful, compact, and reliable. There is a global trend of replacing mechanical linkages and actuator systems with electrical controls and actuators.

In the automotive field, the increasing infusion of electrical systems is observed. The popularisation of anti-lock braking systems (ABS) and traction control systems have encouraged further developments such as the introduction of drive-by-wire. Part of the appeal is that a drive-by-wire system replaces mechanical linkages with electrical controls, thereby simplifying assemblies, increasing design flexibility, enhancing driver controls, improving crashworthiness and environmental impact. Furthermore, drive-by-wire may facilitate better coordinated vehicle dynamics controllers, efficient regenerative braking, and may lead to semi-autonomous driving.

The future brake-by-wire systems may include electromechanical brakes (EMBs). Through replacement of the hydraulic amplifier with an electric motor, the response time of an EMB may be improved over a conventional hydraulic brake. This leads to better ABS performance, shorter stopping distances, and meliorable soft-stop functionality.

The electromechanical brake control problem we deal with in this work is at the servo control level. Complicating the servo controller design is the EMB has a nonlinear response arising from sources such as actuator saturation, friction and nonlinear stiffness. Earlier attempts at EMB control used cascaded proportional-integral (PI) control architectures and ignored the system nonlinearity [Schwarz et al., 1998].

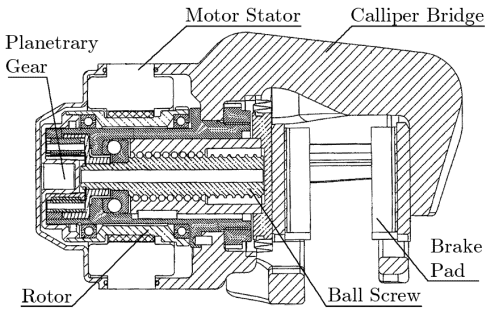

Fig. 1. Cross section of the prototype EMB used in this work (International Publication Number: WO 2005/124180 A1).

The performance of the cascaded PI controller may be improved by plant linearisation, through gain scheduling, friction compensation, and feedback linearisation as shown in [Line et al., 2006].

Additional improvements were observed through the use of a linear unconstrained model predictive control (MPC) [Line, 2007]. Plant linearisation is required in this approach, while actuator constraints are handled by a dynamic current limiter, whereby the applied upper and lower bounds are functions of motor speed and maximum permissible motor current. Although this linear MPC approach resulted in faster transients than observed with the PI controlled system, a drawback of this approach was some controller detuning relative to a full MPC system (that could not be implemented in real time) was required to avoid excessive torque demand.

[1] Email: c.lee33@pgrad.unimelb.edu.au

In addition, the performance of linear MPC is directly related to the quality of the plant linearisation. In the case of [Line, 2007], linearisation of friction and nonlinear stiffness were posed as different subproblems, each of which has to be solved individually. To avoid plant linearisation, it is therefore desirable to conceive an alternative controller design. Moreover, it would be ideal if the controller design process could be fully automated, simply by defining a required performance criterion. Nonlinear constrained MPC offers a potential route to achieve this objective.

Despite advances in computing power, nonlinear constrained MPC is traditionally restricted to slow sampling rate and high performance computers. Real-time implementation requires time-consuming optimisation to be solved online, which is often impractical for automotive applications. Recently, [Bemporad et al., 2002] suggested that the control solution for the linear quadratic regulation problem can be found by offline pre-computation, with the aid of multiparametric programming techniques. The control law obtained offline is in piecewise affine form, and is stored for online implementation. The online implementation is performed by a lookup table method, with the search space as plant states and output as the corresponding control gain. Such an approach can be extended to tracking problems. The corresponding control law (in the form of plant input deviation) will be a function of plant states, reference, and previous input. An explicit MPC control solution for a nonlinear constrained plant is reported in [Johansen, 2004], where an approximate optimum solution is obtained from multiparametric nonlinear programming. The implementation of explicit MPC to another problem in the automotive field is found in [Giorgetti et al., 2006].

This paper extends the prior work of [Line, 2007]. Inspired by the recent developments in explicit MPC [Bemporad et al., 2002], a constrained nonlinear MPC for the EMB is synthesised, and its corresponding explicit nonlinear control law is computed and stored in a table which is accessed online (Section 3). In order to investigate the effect of model parameter variation on control performance, the sensitivity of the explicit solution is evaluated with friction and stiffness variation (Section 4). Furthermore, online adaptation to account for stiffness variation is also included in the EMB controller.

2. EMB MODEL

Versions of simplified EMB models may be found in [Schwarz et al., 1998, Roberts et al., 2003]. In this paper, analysis is undertaken using the experimentally validated EMB model described in [Line, 2007]. This lumped parameter model comprises a simplified motor model and accounts for the nonlinear friction and stiffness characteristics. With appropriate simplifications, the EMB model has an improved simulation efficiency. This is important since it will be used for iterative numerical optimisation during explicit MPC control law computation.

The EMB model describes an electromechanical disk brake with a single motor drive. It comprises lumped inertia, stiffness, and damping about the motor rotation axis. A torque equation is considered about the motor rotation axis, $J\ddot{\theta} = T_m - T_L - T_F$, where J, θ, T_m, T_L, and T_F represent the effective moment of inertia, motor angular position, motor torque, load torque, and friction torque respectively. With the motor quadrature current i_q, motor torque constant K_t, brake clamp force F_{cl}, and gear ratio N, the motor torque and load torque can be calculated with $T_m = i_q K_t$ and $T_L = F_{cl} N$ respectively.

Table 1. EMB model parameters [Line, 2007].

Symbol, Description	Value	Unit
K_t, Motor torque constant	0.0697	Nm/A
T_s, Static friction torque	0.0379	Nm
D, Viscous friction coefficient	3.95×10^{-4}	Nms/rad
C, Coulomb friction torque	0.0304	Nm
G, Friction torque coefficient	1.17×10^{-5}	Nm/N
N, Gear ratio	0.0263	mm/rad
J, Moment of inertia	0.2906×10^{-3}	kgm^2

The nonlinear friction torque is

$$T_F = \begin{cases} D\dot{\theta} + (C + GF_{cl})\,\mathrm{sgn}(\dot{\theta}) & \text{if } |\dot{\theta}| > \epsilon, \\ T_E & \text{if } |\dot{\theta}| < \epsilon \text{ and} \\ & |T_E| < (T_s + GF_{cl}), \\ (T_s + GF_{cl})\,\mathrm{sgn}(T_E) & \text{otherwise,} \end{cases}$$

where the friction model parameters D, C, G, and T_s are the viscous friction coefficient, load-independent Coulomb friction torque, load-dependent friction torque coefficient, and load-independent static friction torque respectively. T_E is the net external non-friction torque. ϵ is a small zero-velocity-bound to implement the Karnopp remedy for zero velocity detection [Olsson et al., 1998].

The nonlinear stiffness characteristic was measured experimentally in [Line, 2007]. With the origin of piston position x_{pp} defined as the contact point between the brake pad and rotor, the stiffness between clamp forces of 0 kN to 40 kN may be approximated as

$$F_{cl} = \begin{cases} -7.23x_{pp}^3 + 33.7x_{pp}^2 - 3.97x_{pp} & \text{if } x_{pp} > 0.121, \\ 0 & \text{otherwise.} \end{cases}$$

Here, the clamp force F_{cl} and the piston position x_{pp} are expressed in kilonewtons and millimeters respectively, where $x_{pp} = N\theta$. The remaining EMB model parameters are tabulated in Table 1.

3. EMB MODEL PREDICTIVE CONTROL

3.1 Problem formulation

The EMB control objective is to track a clamp force command by adjusting the motor current subject to actuator limits on the motor current and speed. The motor current constraints $i_{q\max}, i_{q\min}$ are ± 40 A and the motor speed constraints $\dot{\theta}_{\max}, \dot{\theta}_{\min}$ are ± 300 rad/s respectively.

In the following, we devise an explicit control law $f : \mathcal{R}^4 \mapsto \mathcal{R}$ for the nonlinear EMB plant, where the change in control action at discrete time step k is a function of the reference $F_{cl}^*(k)$, states $x(k) = [F_{cl}(k), \dot{\theta}(k)]$ and the previous control input $i_q(k-1)$, i.e.

$$\Delta i_q(k) = f\left(F_{cl}^*(k), x(k), i_q(k-1)\right). \qquad (1)$$

Clamp force F_{cl} is a function of the motor position θ, i.e. $F_{cl} = g(\theta)$, as described in Section 2. The control input at time step k is then given by $i_q(k) = i_q(k-1) + \Delta i_q(k)$.

The nonlinear constrained MPC problem at time step k may be defined as

$$\begin{aligned}\min_{\Delta i_q} \quad & (e_f(k+H_p))^2 P + \sum_{i=1}^{H_p-1} (e_f(k+i))^2 Q \\ & + \sum_{i=0}^{H_u} (\Delta i_q(k+i))^2 R, \qquad (2)\\ \text{s.t.} \quad & e_f(k+i) = F_{cl}^*(k+i) - F_{cl}(k+i), \\ & F_{cl}(k+i) = g(\theta(k+i)), \qquad i = 1,\ldots,H_p, \\ & \Delta i_q(k+i) = i_q(k+i) - i_q(k+i-1), \quad i = 0,\ldots,H_u, \\ & \theta(k+l) \geq 0, \\ & \dot{\theta}_{\min} \leq \dot{\theta}(k+l) \leq \dot{\theta}_{\max}, \\ & i_{q\min} \leq i_q(k+l) \leq i_{q\max}, \qquad l = 1,\ldots,H_p.\end{aligned}$$

Equation (2) finds the optimal control trajectory to minimise a quadratic cost on the trajectory error e_f to the prediction horizon H_p, change in control Δi_q to control horizon H_u, and a terminal cost on tracking error. The sampling rate is 0.004 s. To avoid reverse over-spinning and damaging the EMB, motor position is constrained to positive values, where zero position represents the contact position of brake pad and rotor. The constraint on motor speed is treated as a soft constraint as some overshoot will not damage the actuator, but is desirable for long term robustness of the device. Conversely, the limit on the motor current is treated as a hard constraint to avoid overheating drive circuits.

The weights P, Q, R are 50, 1, and 30 respectively; and the prediction and control horizons H_p, H_u are 15 and 2 respectively. The weights are chosen such that at the beginning of a full brake application (0 kN to 30 kN step), more than 95% of the cost is related to the tracking error; and at the steady state, more than 95% of the cost is related to the control deviation. The choice of prediction horizon is made such that at least half of the rise time of a full brake manoeuvre is covered by the prediction. The choice of control horizon is a balance between performance and optimisation speed. In the case where maximum optimisation iteration is reached or there is no feasible solution found, the maximum allowable current deviation is chosen.

3.2 Explicit control law and control performance

The domain of the explicit control law (1), dom (f) is four dimensional ($F_{cl}^*(k)$, $\dot{\theta}(k)$, $F_{cl}(k)$, $i_q(k-1)$); and its range is one dimensional ($\Delta i_q(k)$). To obtain the control law (1), dom (f) is discretised into a grid. At each node of the grid, (2) is solved using MATLAB `fmincon` function. `fmincon` uses a sequential quadratic programming (SQP) algorithm to find the solution that minimises an objective function (such as (2)) with a penalty on constraint violation. Figure 2 shows the optimum current deviation $\Delta i_q(k)$ as a function of clamp force $F_{cl}(k)$, motor speed $\dot{\theta}(k)$ and motor current $i_q(k-1)$, whereby the clamp force reference $F_{cl}^*(k)$ is fixed at 13 kN. The discretised grid of dom (f) consists of 31 sections of clamp force reference F_{cl}^* from 0 kN to 30 kN (inclusive), 34 sections of clamp force F_{cl} from 0 kN to 33 kN, 23 sections of motor speed from -330 rad/s to 330 rad/s, and 26 sections of motor current i_q from -40 A to 40 A.

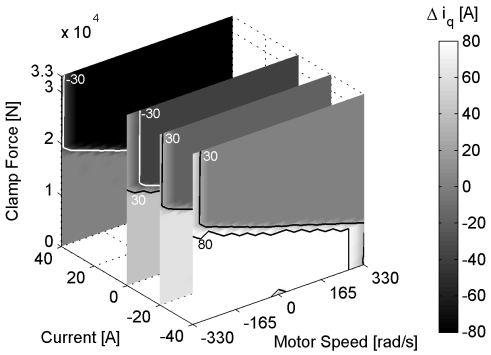

Fig. 2. Optimum current deviation Δi_q as a function of clamp force, motor speed and motor current, whereby the clamp force reference is fixed at 13 kN. The magnitude and contours of the control law are shown on planes $i_q = (-40, -20, 0, 40)$ A.

Online implementation of the control law (1) is achieved using a lookup table. A binary search method is utilised to locate the optimal deviation in control action $\Delta i_q(k)$ for a particular clamp force command $F_{cl}^*(k)$, states (motor speed $\dot{\theta}(k)$, clamp force $F_{cl}(k)$), and the previous control input $i_q(k-1)$.

The step performance and sinusoidal tracking of the explicit nonlinear MPC is compared with the linear MPC reported in [Line, 2007]. The linear MPC was synthesised with prediction and control horizons of 38 and 3 steps respectively. The control cost weighting pair of tracking error and input deviation were tuned as 1 and 75 respectively. Actuator constraints are dealt by using a dynamic current limiter, whereby upper and lower bounds are functions of motor speed and maximum permissible motor current. It is noted that the prediction and control horizons for the explicit nonlinear MPC are chosen shorter than the linear MPC horizons for faster optimisation.

To compare the MPC algorithms, large step manoeuvre and sinusoidal small manoeuvre are chosen as test cases. The large step manoeuvre corresponds to a full brake application (0 kN to 30 kN step) in emergency braking, while the sinusoidal small manoeuvre of 8 Hz corresponds to ABS braking. A faster step response improves reaction time in emergency braking and may reduce stopping distance. Moreover, a better tracking for the 8 Hz sinusoidal reference leads to improvement in ABS performance, thereby reduces wheel lockup and enhances vehicle dynamic stability.

Figure 3 shows the performance comparison of explicit nonlinear MPC and linear MPC. The performance of the two controllers is comparable, in fact, the explicit MPC has a slightly faster step response and lower attenuation level for sinusoidal response. The rise time for large clamp force step trajectories is limited by the EMB hardware design, while tracking performance for small trajectories depends on the controller's ability to handle EMB nonlinearities. In the case of sinusoidal tracking, the motor current trajectory of the explicit nonlinear MPC "chatters" due to the control law interpolation error. However, it is noted that the explicit nonlinear MPC for EMB implementation is simpler, without the need of model linearisation.

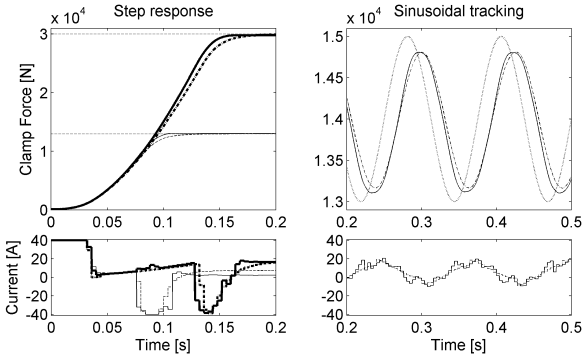

Fig. 3. Clamp force tracking of 13 kN step and 8 Hz 14±1 kN sinusoidal reference (dotted) for linear MPC (dash) and explicit nonlinear MPC (solid).

Table 2. Simulation time for 0.2 s of 13 kN clamp force step responses with different types of MPC and without a controller.

MPC Algorithms	Simulation Time [s]
Online nonlinear MPC	255
Explicit nonlinear MPC	0.177
Linear MPC	0.200
Without controller	0.104

Simulation time for the online nonlinear constrained MPC, explicit nonlinear constrained MPC and linear unconstrained MPC is tabulated in Table 2, in which the online nonlinear constrained MPC optimises (2) at each time step to determine the optimum control during simulation. The simulation scenario is 0.2 s of 13 kN step clamp force response, and is run on a 2.8 GHz Pentium 4 machine. It is observed that the online MPC requires the longest simulation time because optimisation procedure is called in each time step. On the other hand, the explicit nonlinear MPC requires the shortest control computation time, 24% less compared with the linear MPC. This is because plant linearisation and calculation for bounds of the dynamic current limiter are required by the linear MPC. Most of the computation time spent on the explicit nonlinear MPC may be on searching for the corresponding control input on the lookup table. In order to reduce the interpolation error of the control input, a finer grid for the control law domain is desired. However, the size of control law lookup table increases as the domain is discretised finer, whereby larger controller memory is needed. Increased size of lookup table may also result in longer search time, in which holds the key for online implementation.

4. MODEL PARAMETER ADAPTATION

4.1 Control performance under parameter variation

The control action of MPC is based upon its internal model of the plant. An inaccurate plant model may induce suboptimal control performance.

Very often in automotive application, components endure extreme conditions such as large temperature deviation and wear during operation. In particular, the EMB is especially prone to variation in friction and stiffness. Therefore, it is necessary to investigate the effect of parameter variation on control performance.

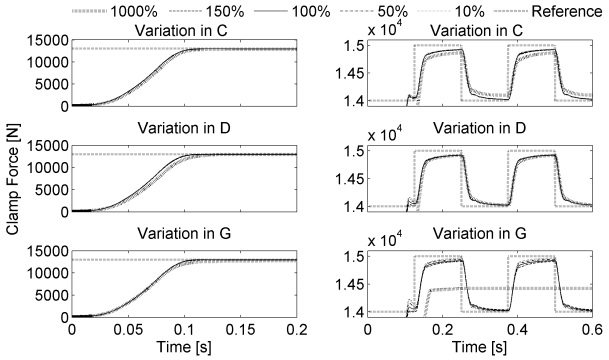

Fig. 4. Clamp force tracking of 13 kN step reference and 4 Hz 14.5±0.5 kN square wave reference for different variation levels of friction parameters, C, D, and G.

To simulate the effect of friction variation on control performance, the friction parameters C, D, G are deviated by 1000%, 150%, 50%, and 10%, from the nominal values tabulated in Table 1. The 1000% and 10% deviations correspond to very extreme cases, while the 150% and 50% deviations correspond to the normal range of deviation. A series of step and tracking responses corresponding to different levels of friction deviation are compared in Figure 4. It is observed that the large step responses are insensitive to friction variations, with maximum steady state error of less than 3% when G is deviated by 1000%, and maximum rise time difference of less than 9% when D is deviated by 1000%. This is expected as the controller is running at the maximum rate, i.e. the control action is close to a "bang-bang" response.

Under small manoeuvres in vicinity of 14.5 kN, the clamp force transient responses are sensitive to variations of load-dependent friction torque coefficient G. Increased G from the nominal leads to under-compensated tracking responses, whereby their amplitudes are attenuated. For the extreme case of 1000% deviation in G, the tracking response is fully attenuated by the large friction torque. On the other hand, decreased G leads to over-compensations. Although over and under-compensations are also shown on the tracking responses for the C and D deviation cases, they are less significant compared with the G deviation case.

The EMB stiffness characteristic is dependent on wear, temperature and types of brake pad. Brake pad constitutes to approximately 28% of the overall compliance, and can exhibit stiffness variation by up to 200% of the nominal value due to wear and temperature variation [Schwarz et al., 1998]. In addition, stiffness may vary as the EMB user replaces brake pads. The stiffness variation may be modelled using a stiffness gain factor α [Schwarz et al., 1999]. Figure 5 shows the clamp force responses as the stiffness is scaled from $\alpha = 0.5$ to $\alpha = 1.5$. It is noticed that the clamp force transient responses are sensitive to stiffness variation. High stiffness leads to overshooting responses, while low stiffness causes slow responses. On one hand, overshooting and slow responses are caused by the over- and under-compensations. On the other hand, slow responses are due to limitation in motor current and speed. It is also noticed that the response at the falling edge of the small manoeuvre is slower as stiffness is reduced. This

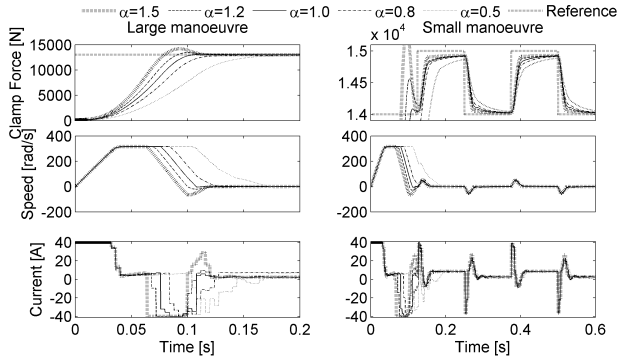

Fig. 5. Clamp force tracking of 13 kN step reference and 4 Hz 14.5±0.5 kN square wave reference for different stiffness characteristics using control law devised for $\alpha = 1$.

may reduce the effect of anti-wheel-lockup during ABS application.

Overall, the steady state errors due to parameters variations are not severe, with the maximum approaching 3% when the load-dependent friction torque coefficient is perturbed by of ten folds. The presence of the past control input in the control loop may act as an integrator such that the steady state errors caused by parameters deviation may be attenuated.

Comparing both large and small manoeuvres, the transient responses are more sensitive to stiffness variation than to friction variation. This is partly because the friction parameters are piecewise affine functions of motor velocity, and the deviations induce an output errors which are linearly dependent on motor speed. On the other hand, the stiffness characteristic is a nonlinear function of motor angular position. Excursion from the nominal stiffness characteristic causes output error with nonlinear behaviour. EMB plant design limitations also affect the transient performance induced by stiffness variation.

4.2 Explicit MPC with model parameter adaptation

The transient clamp force response is sensitive to stiffness variation. In order to obtain optimum performance, it is desirable to adapt the optimum control according to the stiffness variation. Stiffness variation can be observed through estimation of the stiffness characteristic proportional gain α, based on measurements of clamp force and motor position.

In order to address stiffness variation, stiffness characteristic proportional gain α is included in the adaptive explicit control law $f_a : \mathcal{R}^5 \mapsto \mathcal{R}$, i.e.

$$\Delta i_q(k) = f_a \left(F^*_{cl}(k), F_{cl}(k), \dot{\theta}(k), i_q(k-1), \alpha(k) \right). \quad (3)$$

To investigate the control law sensitivity, α is varied by $\pm 20\%$ from the nominal stiffness ($\alpha = 1$). The sensitivity of control law on α is defined as $\Delta^2 i_q = \Delta i_{q,\alpha} - \Delta i_{q,\alpha=1}$. The sensitivity of control surface at $F^*_{cl} = 13$ kN and $i_q = 40$ A is shown in Figure 6. It is observed that Δi_q is only sensitive at a ridge on the $\dot{\theta} - F_{cl}$ plane, in the vicinity of clamp force reference level and motor speed limits. For lower stiffness, the optimum Δi_q is higher (than the nominal) as the clamp force increases to the reference

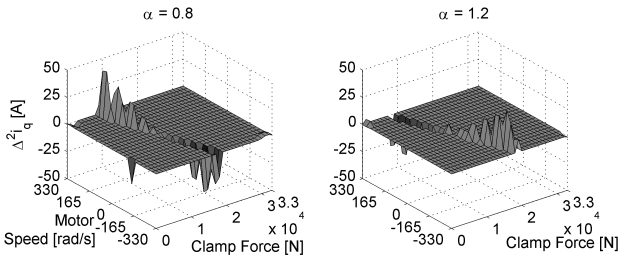

Fig. 6. Sensitivity of control surface at $F^*_{cl} = 13$ kN and $i_q = 40$ A due to variation in stiffness characteristic.

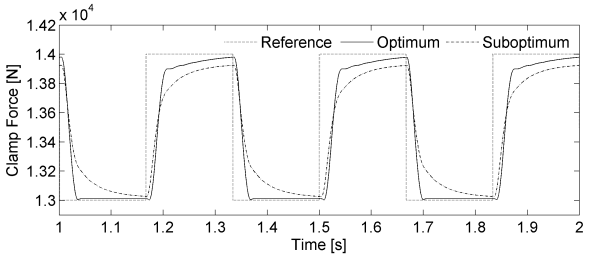

Fig. 7. Simulated 3 Hz square wave tracking comparing the optimum and suboptimum control law (optimum for $\alpha = 1$) on a perturbed EMB with halved stiffness.

and the motor speed increases to the upper limit, while Δi_q is lower as the clamp force is larger than the reference and motor speed decreasing to the lower limit. This means that in lower stiffness, the optimum controller drives the motor close to its velocity limits for longer period in order to reach the reference. The opposite is observed in the higher stiffness case, where by the optimum controller drives the motor close to the velocity limits for shorter period to avoid overshoot.

An adaptive optimum controller may be beneficial for increasing the ABS performance. Very often in ABS applications, clamp force reference drop abruptly as wheel slip is detected to avoid wheel lockup, thereby increasing steerability and reducing stopping distance. Depending on the the wheel slip conditions, the frequency of wheel lockup is in the range of 2 Hz to 8 Hz. To test the performance of the new adaptive explicit control law on a small manoeuvre with stepwise reference, a 3 Hz square wave of 1 kN steps from 13 kN is chosen as the test case, as shown in Figure 7. On a perturbed EMB with halved stiffness, the rise time of the optimum control decreased approximately 75%. Approximately 8% tracking error at the end of the step is found in the suboptimum controller. Accurate tracking for small manoeuvre is important for fine brake torque control. On the falling edge of the step, the optimum controller is more responsive than the subtoptimum, in which the time taken to reach the 10% amplitude from 90% reduced 80%. The responsive performance on the falling edge may decrease wheel lockup during ABS applications.

4.3 Online stiffness characteristic estimation

Online stiffness characteristic estimation is studied in [Schwarz et al., 1999, Lam et al., 2007]. The stiffness characteristic variation is observed by estimating a proportional gain α using recursive least squares (RLS) algo-

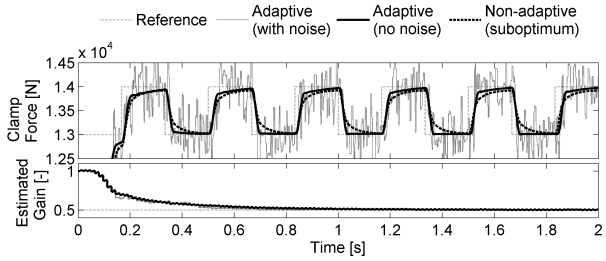

Fig. 8. Simulated 3 Hz tracking comparing the fixed suboptimum and adaptive MPC on an EMB with halved stiffness. Stiffness estimation with and without $N(0, 1.2 \times 10^5)$ measurement noise is shown.

rithm. However, estimation performance under measurement noise were not considered in these papers.

We propose an EMB stiffness characteristic estimation algorithm based upon Robbins-Munro algorithm [Robbins and Munro, 1951]. The Robbins-Munro algorithm is a stochastic approximation (SA) root finding method, analogous to the deterministic gradient descent method. Measurement noise is considered in this method.

Estimation of the stiffness characteristic proportional gain α can be posed as an optimisation problem, minimising the quadratic function of estimation error $Y = (\hat{F}_{cl} - F_{cl})^2$, where $\hat{F}_{cl} = \hat{\alpha} \cdot F(\theta)$. Here, $\hat{F}_{cl}$ is the estimated clamp force, $\hat{\alpha}$ is the estimated stiffness characteristic proportional gain, and $F(\theta)$ is the stored nominal stiffness characteristic as a function of motor angular position. F_{cl} is the clamp force measured using force sensors in the EMB.

Due to sensor noise, F_{cl} measurements may be contaminated. Therefore, the observable estimation performance criterion is the loss function, $L = Y + \varepsilon$, where ε is the effective stochastic noise with zero mean.

Stiffness characteristic proportional gain α at time step $k+1$ can be approximated by the general recursive procedure for SA [Spall, 2003, Section 6.3], $\hat{\alpha}_{k+1} = \hat{\alpha}_k - a_k \hat{g}_k(\hat{\alpha}_k)$, where the gradient $\hat{g}_k$ can be approximated using one-sided finite difference method $\hat{g}_k(\hat{\alpha}_k) = \frac{L(\hat{\alpha}_k + c_k) - L(\hat{\alpha}_k)}{c_k}$. At the beginning of a 0 kN to 30 kN step trajectory, the order of magnitude for the gradient $\mathcal{O}(\hat{g}_k) = 10^8$. Using the guidelines provided in [Spall, 2003, Section 6.6], the following gains are obtained; $a_k = \frac{5 \times 10^{-10}}{(1+k+50)^{0.602}}, c_k = \frac{0.01}{(1+k)^{0.101}}$. $\hat{\alpha}$ is updated in 0.008 s intervals. Explicit implementation of the algorithm would result in decreasing the gains with time to provide convergence of the estimation. However, in practical application where time varying parameters are likely, fixed gains can be used to provide a tracking capability.

Simulation results for the adaptive explicit nonlinear MPC and online stiffness characteristic estimation are shown in Figure 8. The estimated stiffness characteristic proportional gain α approaches the optimum value at 0.5 despite noisy measurement, while improving EMB tracking.

5. CONCLUSIONS AND FUTURE WORK

An explicit nonlinear MPC for an EMB is proposed that avoids plant linearisation and thus simplifies the controller implementation. Simulations show that 24% reduction in computation time is achieved in the explicit MPC compared to the existing linear MPC, with marginally better performance on demanding brake maneouvres. It was observed the tracking performance of the explicit MPC deteriorates under stiffness variation, and so adaptation of the stiffness parameter was incorporated into the explicit nonlinear control law resulting in a rise time reduction of approximately 75% for a 1 kN square wave trajectory. Responsive performance on the falling edge of the steps is also observed, by which is important to reducing wheel lockup in ABS applications. Further work will include improved domain space discretisation, so that interpolation error is reduced for the control law lookup table, while also reducing memory requirements. Experimental validation will also follow in the near future.

REFERENCES

A. Bemporad, M. Morari, V. Dua, and E. N. Pistikopoulos. The explicit linear quadratic regulator for constrained systems. *Automatica*, 38(1):3–20, January 2002.

N. Giorgetti, G. Ripaccioli, A. Bemporad, I. V. Kolmanovsky, and D. Hrovat. Hybrid model predictive control of direct injection stratified charge engines. *IEEE/ASME Transactions on Mechatronics*, 11(5):499–506, October 2006.

T. A. Johansen. Approximate explicit receding horizon control of constrained nonlinear systems. *Automatica*, 40(2):293–300, February 2004.

D. Lam, C. Line, and M. C. Good. Electromechanical brake clamp force estimation. In *Proceedings 14th International Conference on Vehicle Dynamics*, Lyon, France, June 2007.

C. Line. *Modelling and control of an automotive electromechanical brake.* PhD thesis, The University of Melbourne, 2007.

C. Line, C. Manzie, and M. C. Good. Electromechanical brake control: limitations of, and improvements to, a cascaded pi control architecture. In *Mechatronics 2006: The 10th Mechatronics Forum Biennial International Conference*, 2006.

H. Olsson, K. J. Åström, C. Canudas de Wit, M. Gäfvert, and P. Lischinsky. Friction models and friction compensation. *European Journal of Control*, January 1998.

H. Robbins and S. Munro. A stochastic approximation method. *The Annals of Mathematical Statistics*, 22(3): 400–407, September 1951.

R. Roberts, B. Gombert, H. Hartmann, and M. Schautt. Modelling and validation of the mechatronic wedge brake. In *21st Annual Brake Colloquium and Exhibition*, October 2003. SAE Technical Paper: 2003-01-3331.

R. Schwarz, R. Isermann, J. Bohm, J. Nell, and P. Rieth. Modeling and control of an electromechanical disk brake. In *International Congress and Exposition*, February 1998. SAE Technical Paper: 980600.

R. Schwarz, R. Isermann, J. Bohm, J. Nell, and P. Rieth. Clamping force estimation for a brake-by-wire actuator. In *International Congress and Exposition*, March 1999. SAE Technical Paper: 1999-01-0482.

J. C. Spall. *Introduction to Stochastic Search and Optimization: Estimation, Simulation, and Control.* Wiley, Hoboken, NJ, 2003. ISBN 0-471-33052-3.